Journal of Molecular Graphics and Modelling 76 (2017) 181–191

Contents lists available at ScienceDirect

Journal of Molecular Graphics and Modelling

journal homepage: www.elsevier.com/locate/JMGM

# Theoretical investigation of the conformational space of baicalin

Juan J. Martínez Medina[a], Evelina G. Ferrer[b], Patricia A.M. Williams[b], Nora B. Okulik[a,*]

[a] Universidad Nacional del Chaco Austral, Cte. Fernández 755, 3700 Roque Sáenz Peña, Chaco, Argentina
[b] CEQUINOR, Dpto. de Química, Facultad de Ciencias Exactas, UNLP. 47 y 115, 1900 La Plata, Argentina

ARTICLE INFO

*Article history:*
Received 24 May 2017
Received in revised form 5 July 2017
Accepted 6 July 2017
Available online 11 July 2017

*Keywords:*
Baicalin
Conformational space
Density functional theory (DFT)
Atoms in molecules (AIM)
Molecular electrostatic potential (MEP)
Frontier molecular orbital (FMO)

ABSTRACT

Flavonoids are a large group of polyphenolic compounds ubiquitously present in plants. They are important components of human diet. They are recognized as potential drug candidates to be used in the treatment and prevention of a lot of pathological disorders, due to their protective effects. Baicalin (7-glucuronic acid 5, 6-dihydroxyflavone) is one of the main single active constituents isolated from the dried roots of *Scutellaria baicalensis* Georgi. The great interest on this flavonoid is due to its various pharmacological properties, such as antioxidant, antimicrobial, anti-inflammatory, anticancer and so on, and its high accumulation in the roots of *S. baicalensis*. The aim of our work was to analyze the geometric and electronic properties of baicalin conformers (BCL), thus performing a complete search on the conformational space of this flavonoid in gas phase and in aqueous solution. The results indicate that the conformational space of baicalin is formed by eight conformers in gas phase and five conformers in aqueous solution optimized at B3LYP/6-311++G** theory level. BCL$a2_{TT}$ and BCL$a1_{TT}$ conformers have low stability in gas phase and very high stability in aqueous solution. This variation is related to a modification in the $\tau_1$ angle that represents the relative position of the glucuronide unit respect to the central rings of the flavan nucleus (A and C). This modification was successfully explained by examining the changes in the hydrogen bond (HB) interactions that occur in the region around the hydroxyl group located in position 6 of ring A. Besides, the molecular electrostatic potential (MEP) and frontier molecular orbital (FMO) analyses indicate that BCL$a2_{TT}$ and BCL$a1_{TT}$ conformers are the most favorable conformers for interacting with positively charged species (such as metal ions) in aqueous media (such as biological fluids).



## 1. Introduction

Flavonoids are a large group of polyphenolic compounds ubiquitously present in plants. There has been an increasing interest in the research on flavonoids because of their various health benefits reported in several epidemiological studies [1]. They are important components of human diet and the main sources are vegetables, such as fruits, seeds, walnuts, aromatic herbs, onions and legumes. Besides, different drinks, such as wine, tea and beer, contain appreciable amounts of flavonoids [1,2]. They are natural polyphenolic multifunctional antioxidants capable of eliminating reactive oxygen species and reactive nitrogen species by scavenging free radicals, chelating metal ions, inhibiting prooxidant enzymes and activating antioxidant and detoxifying enzymes. They are recognized as potential drug candidates to be used in the treatment and prevention of a lot of pathological disorders [2,3]. Their beneficial properties are ascribed to their antioxidant activity that depends on the number and position of the hydroxyl moieties. However, the wide variety of biological activities of flavonoids is not limited to their antioxidant properties [4]. The main structure of flavonoids is composed by the flavan nucleus (2-phenyl-1-benzopyran-4-one) containing 15 carbon atoms arranged in 3 rings named as A, B and C, where the bridge with 3 carbon atoms is usually cyclized with oxygen [2]. Depending on the degree of oxidation of the γ-pyranone ring, they can be categorized into different subclasses, such as flavones, flavonols and flavanones [4].

Herbal medicine has been practiced in China and other countries for centuries. Baicalein and baicalin are two of the main bioactive compounds found in the traditional Chinese medicinal herb Baikal skullcap (*Scutellaria baicalensis* Georgi). This plant has been used for centuries in traditional Asian medicine and is increasingly being sold in the United States and throughout the Europe [5]. It is cultivated in Poland and the extract from its roots is employed in European pharmaceutical and food industry [6].

Baicalin (7-glucuronic acid 5, 6-dihydroxyflavone) is one of the main single active constituents isolated from the dried roots of *S. baicalensis* and its aglycone form is called baicalein [7]. It is regarded as the marker compound for quality control of over 100 examples

* Corresponding author.
*E-mail address:* noraokulik@gmail.com (N.B. Okulik).

http://dx.doi.org/10.1016/j.jmgm.2017.07.007
1093-3263/

of compound preparations in Chinese Pharmacopoeia [8]. The great interest on this flavonoid is due to its various pharmacological properties and its high accumulation (20%) in the roots of *S. baicalensis* [6,7]. Several studies have demonstrated that baicalin exhibits various biological activities, such as antioxidant, anti-inflammatory, anticancer, hepatoprotective, antibacterial, antiviral [9], antifungal [10], cardioprotective [11], photoprotective [12], antiabortive [13], anxiolytic [14] and immunosuppressive [15]. Moreover, baicalin has showed beneficial effects on several diseases model, such as pancreatitis, obesity, diabetes [9], rheumatoid arthritis [16], asthma [17], androgenetic alopecia [18], Parkinson [19] and Alzheimer [20].

Previous reports have focused on physicochemical properties and pharmacokinetics of baicalin. Zhao et al. [7] have examined marketed preparations of this flavonoid (including capsules and tablets) and they found that the low oral bioavailability may be attributed to the formation of intramolecular hydrogen bonds (IMHB) that result in a poor solubility in water. Baicalin is moderately absorbed in the stomach and poorly absorbed in the small intestine and colon. On the contrary, its aglycone form (baicalein) is well absorbed in the gastrointestinal tract [7]. After oral administration, baicalin is converted to baicalein by b-glucuronidase of intestinal bacteria and then is absorbed and transported to liver. In the liver microsomes, baicalein is transformed into other metabolites by uridine 5′-diphospho-glucuronosyltransferase. This metabolites are 7-*O*-glucuronide-6-methoxyl-5-hydroxyflavone, 6-*O*-glucuronide-5,7dihydroxyflavone and mainly 7-*O*-glucuronide-5,6-dihydroxyflavone (baicalin) [21].

It is acknowledged that computational chemistry can provide insight into the structures and properties of pharmaceuticals at the atomic level, assist the interpretation of experiments and help to develop working hypothesis for further experimental work [22]. This fact highlights the importance of the theoretical studies, and the usefulness of progress in our detailed knowledge of conformational space of baicalin. Few reports have focused on theoretical investigations of this flavonoid. Dai et al. [23] have studied some structural and electronic properties of this flavonoid at B3LYP/6-31G* theory level and Wolniak et al. [6] have performed calculations of nuclear magnetic resonance (NMR) parameters. Nevertheless, these reports are based on a little number of conformers selected by its energy stability and the calculations were carried out without considering the solvent effect. To our knowledge, no study of the conformational space of this flavonoid has been reported in the literature. The aim of our work was to analyze the geometric and electronic properties of baicalin conformers (BCL), thus performing a complete search on the conformational space of this flavonoid in gas phase and in aqueous solution. Besides, studies on the hydrogen bond (HB) interaction by atoms in molecules (AIM), molecular electrostatic potential (MEP) and frontier molecular orbital (FMO) were carried out.

## 2. Computations

The X-ray diffraction data of baicalin have been previously reported [23]. This structure was employed as starting point to analyze the conformational space of this flavonoid. The profiles of the potential energy surfaces were obtained performing three rigid scan rotating procedures using the semi-empirical method called PM3 [24,25]. Then, the minimum energy conformers were reoptimized with totally relaxed geometries using tools from density functional theory [26–28] as implemented in the GAUSSIAN 09 program package [29]. These optimization procedures were carried out employing the *ab initio* method known as B3LYP [30] combined with different basis sets in gas phase and in aqueous solution.

Fig. 1 shows the numbering and principal angles used for the analysis of the conformational space of baicalin. The first scan was performed taking into account the rotation of the dihedral angles ($\tau_1$) = C8—C7—O7—C1″, ($\tau_2$) = O1—C2—C1′—C2′ and ($\tau_3$) = O6$_c$″(carbonyl)–C6″—C5″O5″ around the bonds C7—O7, C2—C1′ and C6″—C5″ in steps of 60°. The $\tau_1$ and $\tau_2$ angles represent the relative position of the glucuronide unit and the ring B respect to the central rings (A and C), respectively. The $\tau_3$ angle configures the position of the acid group in the glucuronide unit. Some of these conformers were selected to be employed in the next step considering the stability order and eliminating the duplicate structures. The second scan was performed taking into account the effects of the rotation around the C—O bonds of the OH substituents at C5 and C6 of ring A and the OH of the carboxylic acid in steps of 90°. These dihedral angles are ($\tau_4$) = C10—C5—O5—H, ($\tau_5$) = C5—C6—O6—H and ($\tau_6$) = C5″—C6″—O6″—H. Some of these conformers were selected

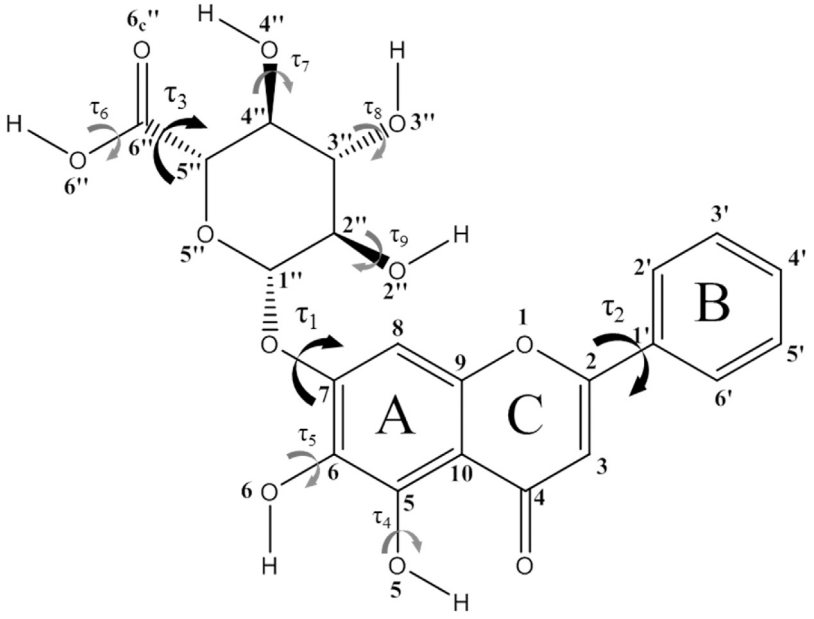


**Fig. 1.** Scheme of the molecule of baicalin. Numbering and principal angles used for the analysis.

to be employed in the next step considering the stability order and geometrical parameters. The third scan was performed taking into account the effects of the rotation around the C—O bonds of the OH substituents in the glucuronide unit in steps of 90°. These dihedral angles are ($\tau_7$) = C5″—C4″—O4″—H, ($\tau_8$) = C4″—C3″—O3″—H and ($\tau_9$) = C3″—C2″—O2″—H.

The primitive structures obtained in the third scan were subsequently reoptimized with totally relaxed geometries using the B3LYP functional combined with two basis sets (3-21G* and 6-31G*). Among these structures optimized employing the 6-31G* basis sets, a few structures were selected and reoptimized at B3LYP/6-31G** theory level. Harmonic vibrational frequencies were calculated at the same theory level to confirm the presence of true minimum energy structures, as well as to perform thermodynamic corrections that are included in all electronic energies reported. Then, conformers with an energy difference relative to the most stable conformer ($\Delta E$) lower than 3 kcal mol$^{-1}$ were further reoptimized (and harmonic vibrational frequencies were calculated) in gas phase using triple zeta valence quality basis set augmented with polarization and diffuse functions (6-311++G**) for all atoms. The reliability of the B3LYP/6-311++G** theory level for this flavonoid has been previously reported [6]. The hybrid B3LYP functional, which is the most popular functional, was originally developed to provide an excellent performance for main-group structures, noncovalent interactions, thermochemistry, kinetic applications, excited states, and transition elements. It has also been demonstrated to provide satisfactory description of solvent effects on the structures and properties of compounds. The diffuse function was included in order to treat the lone electron pairs properly and it is a clear requirement to adequately describe hydrogen bonded systems [22].

Although the theoretical results of an isolated molecule are very useful for determining the intrinsic properties of the system free of any kind of interaction, such results can be compared with experimental data in only a few cases, since most assays are performed in solution. In this context, and considering that water is the main component of biological fluids, it is necessary to take into account the effect of the aqueous solvent [31,32]. The conformers optimized in gas phase were further reoptimized and harmonic vibrational frequencies were calculated at the same theory level (B3LYP/6-311++G**), but considering the effect of the aqueous solvent. Tomasi's polarizable continuum model (PCM) [33] was employed considering the dielectric constant of water ($\varepsilon$ = 78.3553). The PCM approach considers that the molecule under study is inside a cavity embedded in a polarizable dielectric, thus allowing solvent modeling by choosing the proper dielectric constant without the explicit inclusion of solvent molecules. This model has proven to be a reliable tool for the description of solute-solvent electrostatic interactions [32]. In this model, the atomic radii of spheres employed to build the molecular cavity were adjusted introducing chemical consideration, such as hybridization, formal charge and first neighbor inductive effect. The effect of the escaped electronic charge outside the cavity was corrected with an additional set of charges on the cavity surface that was distributed according to the solute electronic density in each point of the surface [22].

After the conformational search was completed, studies of HB interactions, MEP and FMO were carried out in the selected conformers. The MEP on the van der Waals surface was obtained using the GAUSSIAN 09 [29], Multiwfn [34], and VMD programs [35]. The isosurface of HOMO and LUMO were rendered using Avogadro software [36] and the calculations of orbital composition were carried out employing Multiwfn software [34]. Besides, HBs interactions were studied and characterized by AIM theory [37]. The topological analysis and the evaluation of local properties were performed with AIMALL software [38] by using the wave functions calculated at B3LYP/6-311++G** theory level.

## 3. Results and discussion

### 3.1. Conformational and structural analysis

The study of the conformational space of baicalin was carried out without any constrains. Seven conformers were selected from the first scan (that involves the $\tau_1$, $\tau_2$ and $\tau_3$ angles) and then were employed in the second scan (that involves the $\tau_4$, $\tau_5$ and $\tau_6$ angles). These conformers were selected considering that the $\tau_2$ angle shows values close to 30°, 90°, 150°, −150°, −90° and −30°. Due to the symmetry of the phenyl group in baicalin (without substituents in ring B), the last three angles represent the same disposition that the first ones. After the second scan, the $\tau_2$ angle value changed in the conformer with $\tau_2$ = 90°. These preliminary results suggest that the perpendicular disposition of the ring B respect to the central rings (A and C) is less probable. These data are consistent with the fact that perpendicular conformations of the flavonoids luteolin and apigenin are associated with high potential barriers [39]. Eleven conformers were selected from the second scan and employed in the third scan (that involves the $\tau_7$, $\tau_8$ and $\tau_9$ angles). After the third scan was completed, twenty two structures were selected and reoptimized with totally relaxed geometries at B3LYP/3-21G* and B3LYP/6-31G* theory levels. The conformers optimized employing the 3-21G* basis sets showed a relevant modification in the $\tau_2$ angle. This dihedral angle that showed values close to −45° or +45° in the primitive structures (selected from the third scan) takes values close to zero after optimization at B3LYP/3-21G* theory level. When these structures were reoptimized employing the 6-31G* basis sets, in some cases the $\tau_2$ angle reverts to the original value, whereas in other cases it takes the opposite one. Previous studies on similar flavonoids have characterized the potential energy curves as a function of the $\tau_2$ angle and their results suggest that the planar structures represent saddle points [39,40]. These facts allowed us to conclude that the B3LYP/3-21G* theory level is not adequate for this system. On the contrary, the conformers optimized employing 6-31G* basis sets preserves the geometrical information related to the disposition of the ring B ($\tau_2$). These findings suggest that the B3LYP/6-31G* theory level results adequate for this system. For the next step, ten structures were selected from the structures optimized employing the 6-31G* basis sets and reoptimized at B3LYP/6-31G** theory level. Harmonic vibrational frequencies were calculated at the same theory level. These structures have been confirmed as minima by the absence of negative frequencies and the thermodynamic corrections were included in all the reported electronic energies (Table 1).

The BCL conformers were named and grouped considering some geometrical aspects. The $\tau_1$ angle (disposition of the glucuronide unit) allowed the classification of BCL conformers into four groups, indicated by *a*, *b*, *c* and *d*, and the average values of this angle in each group are −39.89°, −125.40°, 119.80° and 4.85°, respectively. Dai et al. [23] reported a $\tau_1$ angle of 106.4°, similar to that we found in the *c* group. They proposed two HBs that contribute to the sandwich-like molecular packing in the solid state. These HBs are C2″—OH···O—C4″ (intramolecular) and C5—OH···O—C6 (intermolecular). Wolniak et al. [6] suggested two possible values of $\tau_1$ angle and one of them (2.8°) is close to the value that we found in the *d* group. The $\tau_2$ angle (disposition of the phenyl group) has only two possible values 20° or −20° (−20° is equal to 160° due to the symmetry of the phenyl group without substituents in ring B) and this fact led us to classify the BCL conformers into the *1* and *2* groups, respectively. The *1* group shows similar $\tau_2$ angle values in comparison with crystallographic data (7.7°) and the dif-

**Table 1**
Energy and characteristic $\tau_1$ and $\tau_5$ dihedral angles for ten minimum energy BCL conformers optimized in gas phase at B3LYP/6-31G** theory level.

| Conformer | $\tau_1$ angle | $\tau_5$ angle | Energy [a] | ΔE [b] | ΔE [c] | Relative population [d] |
|---|---|---|---|---|---|---|
| BCL$a2_{CT}$ | −37.47 | −9.33 | −1027970.8470 | 0.00 | 0.00 | 13.46 |
| BCL$a1_{CT}$ | −37.52 | −9.65 | −1027970.4618 | 0.39 | 0.39 | 12.49 |
| BCL$a1_{TT}$ | −42.24 | −163.80 | −1027969.8970 | 0.95 | 0.95 | 9.20 |
| BCL$a2_{TT}$ | −42.32 | −164.05 | −1027969.8782 | 0.97 | 0.97 | 9.58 |
| BCL$b1_{CC}$ | −124.32 | −0.57 | −1027970.7987 | 0.05 | 0.00 | 13.22 |
| BCL$b2_{CC}$ | −126.49 | −1.80 | −1027970.0407 | 0.81 | 0.76 | 15.01 |
| BCL$c1_{CC}$ | 126.21 | 0.03 | −1027969.5450 | 1.30 | 0.00 | 10.49 |
| BCL$c1_{CT}$ | 113.39 | −0.27 | −1027968.4983 | 2.35 | 1.05 | 9.18 |
| BCL$d2_{TT}$ | 9.66 | −171.22 | −1027967.0650 | 3.78 | 0.00 | 5.16 |
| BCL$d1_{TT}$ | 0.05 | −168.19 | −1027964.9943 | 5.85 | 2.07 | 2.21 |

[a] Energy calculated at B3LYP/6-31G** theory level and corrected by zero point energy (ZPE), expressed in kcal mol$^{-1}$.
[b] Energy difference relative to the most stable conformer, expressed in kcal mol$^{-1}$.
[c] Energy difference relative to the most stable BCL conformer in each group, expressed in kcal mol$^{-1}$.
[d] Relative Population percentage calculated by Boltzmann, expressed in%.

ferences may be satisfactory explained considering the π-π staking interactions between the different molecules present in the crystal [23], but not on the isolated molecules. Previous reports for similar flavonoids revealed that the potential energy curves of the $\tau_2$ angle are almost flat in the region of ±40° [41], ±30° (±15°) at MP2 (B3LYP) theory level [39]. They suggested that structures with $\tau_2$ angle close to 0 represent a planar saddle points between two stable structures with a small negative frequency associated to a torsional mode around C2—C1′ bond. Moreover, Amat el al. [39] suggested the presence of both structures (*1* and *2*) with an almost free oscillation of phenyl B ring in a range of ±20° around the planar structure. Rossi et al. [42] reported the crystallographic data of the aglycone of baicalin (baicalein) and proposed a planar conformation with a $\tau_2$ angle of 8.2°. However, the analysis of the factors that affect the planarity of the flavone framework has been earlier discussed by this group and they concluded that the lowest potential energy corresponds to a nonplanar conformation in with a $\tau_2$ angle equal to 22.8°. This intermediate torsion angle, which is similar to that we found in baicalin, represents a balance between the attractive interaction from a planar structure that provides the framework for a more extensive mesomeric effect and the repulsive steric interactions that may result from the two ortho hydrogen atoms. Marković et al. [41] reported that the absolute minima in $\tau_2$ angle of baicalein were found at 21.00° and at 158.95° and the C2—C1′ bond is in the chromone plane and has a length of 1.473 Å, in accordance with our data for baicalin. The $\tau_3$ angle (position of the acid group) did not allow another classification. The average values of this angle in the *a*, *b*, *c* and *d* groups are −122.46°, −151.65°, −169.48° and −103.44°, respectively. On the other hand, the possible arrangements of the OH groups explored in the second scan ($\tau_4$, $\tau_5$ and $\tau_6$) allowed another classification of the BCL conformers, indicated by the subscripts C or T. This designation referred to syn (cis) and anti (trans) configurations of O5—H, O6—H and O6″—H bonds relative to C10—C5, C5—C6 and C5″—C6″bonds, respectively. The average values of $\tau_4$, $\tau_5$ and $\tau_6$ angles were close to 0° (cis) or close to 180° (trans). Taking into account that the configuration of the OH group located in the position 5 of the ring A ($\tau_4$) was always cis, the configuration of this angle was not included in the nomenclature of the BCL conformers. The subscripts C or T in the nomenclature of the BCL conformers indicate the configuration of the $\tau_5$ (first subscript) and $\tau_6$ (second subscript) angles. The fact that the configuration of the $\tau_4$ angle was always cis may be explained by the formation of an IMHB between the hydrogen of the OH group located in position 5 of ring A and the oxygen of the carbonyl group located in position 4 of ring C. Wolniak et al. [6] have previously reported this IMHB for baicalin, baicalein and wogonoside based on NMR spectroscopy evidence. They characterized the C5—OH···O=C4 interaction by $^{13}$C NMR in solution and solid state and reported that the chemical shifts indicate the presence of this IMHB in both phases. Besides, Marković et al. [41] suggested that the formation of the C5—OH···O=C4 bond has a stabilizing effect in baicalein molecule. Nevertheless, this HB interaction is absent in the crystal of baicalin because the OH located in position 5 has trans configuration and the hydrogen of this group is involved in an intermolecular HB with the oxygen of the OH located in position 6 (also in trans configuration) of an adjacent baicalin unit [23]. The $\tau_7$, $\tau_8$ and $\tau_9$ angles are not represented in the nomenclature, but were taken into account to select the lower energy BCL conformers.

The energy difference between the structures of the *a*, *b* and *c* groups with respect to *d*, lead us to not consider the latter in the deeper study performed below. The geometries of the eight conformers with a ΔE value lower than 3 kcal mol$^{-1}$ represented by the *a*, *b* and *c* groups were refined performing reoptimizations in gas phase using the B3LYP method and triple zeta valence quality basis set augmented with polarization and diffuse functions. These conformers showed no significant geometrical differences respect to the starting structures (Table 2). The average values of the $\tau_1$ angle are −35.31°, −122.07° and 122.17° in the *a*, *b* and *c* groups,

**Table 2**
Energy and characteristic $\tau_1$ dihedral angle for eight BCL conformers optimized in gas phase at B3LYP/6-311++G** theory level.

| Conformer | $\tau_1$ angle | Energy [a] | ΔE [b] | ΔE [c] | Relative population [d] |
|---|---|---|---|---|---|
| BCL$a2_{CT}$ | −34.48 | −1028253.8344 | 0.00 | 0.00 | 16.51 |
| BCL$a1_{CT}$ | −33.96 | −1028253.5194 | 0.32 | 0.32 | 13.21 |
| BCL$a1_{TT}$ | −33.99 | −1028252.1050 | 1.73 | 1.73 | 8.50 |
| BCL$a2_{TT}$ | −38.83 | −1028252.0234 | 1.81 | 1.81 | 9.10 |
| BCL$b1_{CC}$ | −121.98 | −1028253.3663 | 0.47 | 0.00 | 11.90 |
| BCL$b2_{CC}$ | −122.16 | −1028253.2552 | 0.58 | 0.11 | 12.59 |
| BCL$c1_{CC}$ | 127.31 | −1028253.1830 | 0.65 | 0.00 | 13.72 |
| BCL$c1_{CT}$ | 117.0289 | −1028252.5009 | 1.33 | 0.68 | 14.47 |

[a] Energy calculated at B3LYP/6-311++G** theory level and corrected by ZPE, expressed in kcal mol$^{-1}$.
[b] Energy difference relative to the most stable conformer, expressed in kcal mol$^{-1}$.
[c] Energy difference relative to the most stable conformer in each group, expressed in kcal mol$^{-1}$.
[d] Relative Population percentage calculated by Boltzmann, expressed in%.

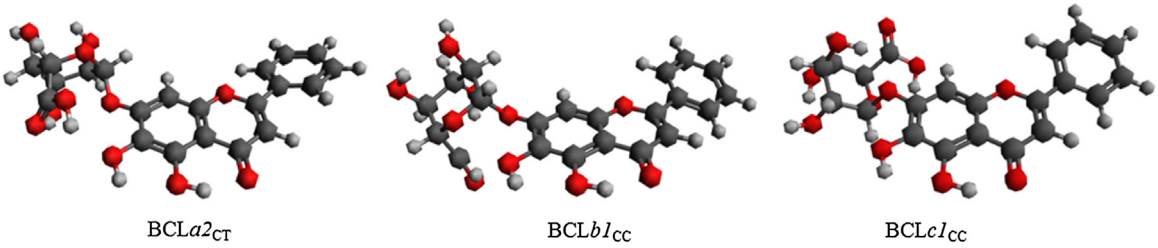


**Fig. 2.** Structures of the most stable BCL conformers optimized in gas phase at B3LYP/6-311++G** theory level in each group.

**Table 3**
Energy and characteristic $\tau_1$ dihedral angle for eight BCL conformers optimized in aqueous solution at B3LYP/6-311++G** theory level.

| Conformer | $\tau_1$ angle | Energy [a] | ΔE [b] | ΔE [c] | ΔE [d] | Relative population [e] |
|---|---|---|---|---|---|---|
| BCL$a2_{TT}$ | 15.10 | −1028272.4520 | 20.43 | 0.29 | 0.00 | 18.99 |
| BCL$a1_{TT}$ | 15.87 | −1028272.4400 | 20.34 | 0.30 | 0.01 | 21.48 |
| BCL$a2_{CT}$ | −34.21 | −1028270.6830 | 16.85 | 2.06 | 1.77 | 6.93 |
| BCL$a1_{CT}$ | −34.74 | −1028270.6290 | 17.11 | 2.12 | 1.82 | 6.99 |
| BCL$b2_{CC}$ | −115.56 | −1028272.7444 | 19.49 | 0.00 | 0.00 | 16.80 |
| BCL$b1_{CC}$ | −101.13 | −1028272.2267 | 18.86 | 0.52 | 0.52 | 13.48 |
| BCL$c1_{CC}$ | 127.66 | −1028270.7514 | 17.57 | 1.99 | 0.00 | 8.44 |
| BCL$c1_{CT}$ | 122.69 | −1028270.0611 | 17.56 | 2.68 | 0.69 | 6.90 |

[a] Energy calculated at B3LYP/6-311++G** theory level and corrected by ZPE, expressed in kcal mol$^{-1}$.
[b] Solution-vacuum energy difference.
[c] Energy difference relative to the most stable conformer, expressed in kcal mol$^{-1}$.
[d] Energy difference relative to the most stable conformer in each group, expressed in kcal mol$^{-1}$.
[e] Relative Population percentage calculated by Boltzmann, expressed in%.

respectively. The $\tau_2$ angle remained unchanged. The average values of the τ3 angle are −122.85°, −154.76° and −163.79° in the *a*, *b* and *c* groups, respectively. Although the energetic order of the conformers is slightly different compared with that determined in the previous step, the most stable conformers involved the *a* and *b* groups. The eight conformers have a ΔE lower than 2 kcal mol$^{-1}$ and this low energetic difference suggests the coexistence of all of these species at room temperature. The relative populations were calculated by the Maxwell-Boltzmann distribution at 298.15 K. The energy difference between the conformers of the *a* group with a cis configuration of the $\tau_5$ angle and that those with a trans configuration led to relative populations of about 30% and 18%, respectively. These results, and the fact that the other six BCL conformers have the cis configuration of the $\tau_5$ angle, indicate that this configuration is more probable and gives more stability to the molecule in the gas phase. Fig. 2shows the most stable conformers in gas phase in each group (BCL$a2_{CT}$, BCL$b1_{CC}$ and BCL$c1_{CC}$).

### 3.2. Effect of aqueous solvent on conformational and structural analysis

The effect of aqueous solvent modified the conformational space of baicalin (Table 3). The reoptimization of the eight conformers previously optimized in gas phase at the same theory level (B3LYP/6-311++G**), but employing the solvent effect, led to five conformers with a ΔE lower than 2 kcal mol$^{-1}$. This low energetic difference suggests the coexistence of these five species at room temperature. The conformational space was reduced to two conformers for the *a* group, two for the *b* group and one for the *c* group. The average values of the $\tau_1$ angle are 15.48°, −108.35° and 125.18° in the *a*, *b* and *c* groups, respectively. The $\tau_2$ angle remained unchanged and the average values of the τ3 angle are −123.53°, −165.75° and −158.72° in the *a*, *b* and *c* groups, respectively. Surprisingly, the two most stable conformers of the *a* group (BCL$a2_{TT}$ and BCL$a1_{TT}$) show a modification in the $\tau_1$ angle (15.48°) in comparison with the conformers BCL$a2_{CT}$ and BCL$a1_{CT}$ (−34.47°). Although these conformers had been characterized like the less stable conformers in gas phase, they show a significant higher stability in aqueous solution compared with those that show a $\tau_1$ angle close to −34°. Moreover, the BCL$a2_{CT}$ and BCL$a1_{CT}$ conformers have a ΔE slightly higher than 2 kcal mol$^{-1}$. These results suggest that the conformers of the *a* group that show a $\tau_1$ angle close to −34° are the most stable conformers in the gas phase, but no in aqueous solution. In an effort to explain this phenomenon, geometrical aspects of HBs and AIM studies were carried out for the conformers of the *a* group in both phases. The conformers of the *b* and *c* groups showed small changes after reoptimization in aqueous medium. The stability order determined in gas phase (*a* > *b* > *c*) changed and the most stable conformer in aqueous solution is BCL$b2_{CC}$ (*b* group). However, the higher stability structures involved the *a* and *b* groups. The energy difference between the conformers of the *a* group with a cis configuration of the $\tau_5$ angle and those with a trans configuration led to relative populations of about 14% and 40%, respectively. Fig. 3 shows the most stable conformers in aqueous solution in each group (BCL$a2_{TT}$, BCL$b2_{CC}$ and BCL$c1_{CC}$). As expected, all structures were more stable in solution than in gas phase, and on average the energy difference for the structures in aqueous solvent and in vacuum was 18.53 kcal mol$^{-1}$.

### 3.3. Geometrical aspects of IMHB

Zheng et al. [43] have previously analyzed the geometrical criteria for assessing the presence of IMHB interactions for apigenin in the gas phase and in the presence of different solvents. The geometrical aspects of HBs were studied for the conformers of the *a* group in both phases (Table 4). The distances between oxygen and hydrogen atoms involved in the HB interaction are in the range of 1.694–2.489 Å (except C6″OH···O—C6 bond in BCL$a1_{TT}$). These values are smaller than the sum of van der Waals atomic radii of hydrogen and oxygen (2.5 Å) [43]. Besides, the values of the angle formed between the oxygen and hydrogen atoms (covalent bounded) and the oxygen atom involved in the HB interaction (O—H···O) are in the range of 111.4–161.6°. These values are among 90–180° that was determined for HBs [43]. These results suggest the presence of IMHB interaction in the selected conformers. It is well known that the geometrical parameters of the HB can reflect


**Fig. 3.** Structures of the most stable BCL conformers optimized in aqueous solution at B3LYP/6-311++G** theory level in each group.

**Table 4**
Geometrical parameters for IMHBs present in the BCL conformers of the *a* group optimized in gas phase and in aqueous solution at B3LYP/6-311++G** theory level.

| Conformer | Atoms pair [a] | Gas phase | | Aqueous solution | |
|---|---|---|---|---|---|
| | | Distance [b] | Angle [c] | Distance [b] | Angle [c] |
| BCL$a1_{CT}$ | H5···O4 | 1.713 | 147.4 | 1.710 | 148.0 |
| | H6''···O6 | 2.231 | 122.4 | 2.462 | 112.3 |
| | H3''···O6c" | 1.889 | 158.5 | 1.871 | 160.8 |
| | H4''···O2'' | 2.224 | 132.4 | 2.056 | 139.8 |
| BCL$a2_{CT}$ | H5···O4 | 1.712 | 147.4 | 1.711 | 148.0 |
| | H6''···O6 | 2.166 | 125.6 | 2.473 | 112.0 |
| | H3''···O6c" | 1.927 | 156.5 | 1.876 | 160.4 |
| | H2''···O4'' | 2.182 | 134.4 | 2.058 | 139.6 |
| BCL$a1_{TT}$ | H5···O4 | 1.712 | 148.4 | 1.694 | 149.5 |
| | H6''···O6 | 2.568 | 111.4 | – | – |
| | H6···O6c" | 2.472 | 121.5 | – | – |
| | H3''···O6c" | 1.847 | 158.3 | 1.866 | 161.6 |
| | H4''···O2'' | 2.184 | 134.4 | 2.034 | 140.2 |
| | H6···O7 | – | – | 2.110 | 113.1 |
| BCL$a2_{TT}$ | H5···O4 | 1.711 | 148.4 | 1.694 | 149.5 |
| | H6''···O6 | 2.489 | 113.3 | – | – |
| | H6···O6c" | 2.331 | 126.7 | – | – |
| | H3''···O6c" | 1.842 | 159.6 | 1.868 | 161.4 |
| | H4''···O2'' | 2.186 | 134.3 | 2.039 | 140.1 |
| | H6···O7 | – | – | 2.112 | 113.0 |

[a] Atoms pair involved in the hydrogen bond interaction.
[b] Distance between oxygen and hydrogen atoms involved in the hydrogen bond interaction (H···O), expressed in angstroms (Å).
[c] Angle between the oxygen and hydrogen atoms (covalent bounded) and the oxygen atom involved in the HB interaction (O—H···O), expressed in grades (°).

its strength. The smaller H···O distance and the larger O—H···O angle, the stronger is the HB [43]. The C5—OH···O=C4 bond is the strongest HB in all BCL conformers and the increase in the H···O distance and decrease in O—H···O angle diminishes the HB strength (Table 4).

### 3.4. Topology of the electronic charge density function

From analysis of the topology of the molecular charge density (ρ), relevant information can be extracted about the molecular structure, whose main characteristics are summarized in the curvatures of the molecular charge density at critical points. AIM theory is based on the analysis of these critical points and has become a powerful tool for characterizing and understanding HB interaction [44]. According to this theory [37], upon formation of a chemical bond between two neighboring atoms, a critical point appears between them. Hydrogen bond, like any other chemical bond, must correspond to the existence of a bond path between the proton donor and the proton acceptor containing the bond critical point (BCP). Besides, the existence of a ring critical point (RCP) within the quasi-ring formed by the HB network is necessary to propose an IMHB interaction [45]. Our data, in agreement with this theory, confirm the existence of IMHB interactions. The electron charge density (ρb), the Laplacian of the charge density ($\nabla^2 \rho_b$), ellipticity ($\varepsilon$) and kinetic energy density ($G_b$) in the BCP were studied for the IMHBs present in the BCL conformers of the *a* group in gas phase and in aqueous solution (Table 5).

Bentz et al. [32] extensively explained the $\rho_b$, $\nabla^2 \rho_b$, $\varepsilon$ and $G_b$ parameters in a previous report. They consider that when the interaction is described by relatively low values of $\rho_b$, $\nabla^2 \rho_b > 0$ and $|l1|/\lambda 3 < 1$ and $G_b > 1$, the same is classified as a closed shell interaction (typical in ionic bonds, hydrogen bonds, and van der Waals interactions), in agreement with our data. Besides, $\nabla^2 \rho_b$ values are all positive and within the range accepted for HB interactions [44]. The AIM topology graphs of BCL$a1_{CT}$ and BCL$a1_{TT}$ conformers optimized in gas phase and in aqueous solution were selected for comparative purposes (Fig. 4). Their homologous structures with the phenyl in −20° show similar AIM topology graphs. The analysis of the graphs revealed that the BCL conformers with a cis configuration of the $\tau_5$ angle show no modification after reoptimization in aqueous medium. On the contrary, the BCL conformers with a trans configuration of the $\tau_5$ angle show relevant modifications in the HB interactions in the region around the OH located in position 6 of ring A (after reoptimization in aqueous medium). These modifications might explain the variation in the $\tau_1$ angle observed after reoptimization in aqueous medium in the BCL conformers with a trans configuration of the $\tau_5$ angle.

The electron charge density is related with the strength of the HB. The higher value of $\rho_b$, the stronger is the HB interaction. The values of $\rho_b$ in BCL conformers are in the range of 0.009–0.049 au, within the range determined for HB interactions [43]. The values of $\rho_b$ for C5—OH···O=C4 bonds are greater than the other HBs, thus suggesting that these bonds are the strongest HBs. The low values of $\rho_b$ (close to 0.009) for C6″—OH···O—C6 and C6—OH···O=C6″ bounds in BCL conformers with a trans configuration of the $\tau_5$ angle indicate that these HBs are very weak. These results are in accordance with those of the study of geometrical aspects of HBs. These findings support the hypothesis that the C6″—OH···O—C6 and C6—OH···O=C6″ bonds are easily broken by the solvent with generation of a new HB with a $\rho_b$ close to 0.02 au (C6—OH···O—C7) in these conformers. The structural modification of BCL conformers with a trans configuration of the $\tau_5$ angle observed in aqueous solution and the consequent variation in the $\tau_1$ angle leading to more stable structures might be explained by these data.

Another parameter of interest is the ellipticity, interpreted as a measure of the anisotropy of the curvature of the electron density in the directions perpendicular to the bond [45]. The $\varepsilon$ is close to zero in a bond with cylindrical symmetry [32]. In general trends, the $\varepsilon$ is close to 0.0 in the HBs of the BCL conformers, thus indicating the cylindrical symmetry of these bonds. Nevertheless, in a few cases the $\varepsilon$ values are close to 0.1 and for the C6—OH···O—C7 bond the $\varepsilon$ values are abnormally higher, thus suggesting that the symmetry of these bonds are less cylindrical.

Previous reports have proposed an IMHB between the H6 and O5 atoms. Wolniak et al. [6] suggested that the structures of baicalein and baicalin with anticlockwise orientation (cis) of OH groups are more probable than those with clockwise orientation (trans), due

**Table 5**
Values of the electroncharge density ($\rho_b$), Laplacian of the charge density ($\nabla^2\ \rho_b$), ellipticity ($\varepsilon$) and kinetic energy density ($G_b$) in the bond critical point for IMHBs present in the BCL conformers of the *a* group optimized in gas phase and in aqueous solution at B3LYP/6-311++G** theory level.

| Conformer | Atoms pair [a] | Gas phase | | | | Aqueous solution | | | |
|---|---|---|---|---|---|---|---|---|---|
| | | $\rho_b$ | $\nabla^2\ \rho_b$ | $\varepsilon$ | $G_b$ | $\rho_b$ | $\nabla^2\ \rho_b$ | $\varepsilon$ | $G_b$ |
| BCL*a1*$_{CT}$ | H5···O4 | 0.047 | +0.130 | 0.016 | +0.038 | 0.047 | +0.132 | 0.021 | +0.039 |
| | H6′′···O6 | 0.015 | +0.053 | 0.111 | +0.012 | 0.010 | +0.037 | 0.325 | +0.008 |
| | H3′′···O6c” | 0.028 | +0.101 | 0.038 | +0.024 | 0.030 | +0.105 | 0.041 | +0.025 |
| | H4′′···O2′′ | 0.016 | +0.053 | 0.103 | +0.012 | 0.022 | +0.075 | 0.059 | +0.017 |
| BCL*a2*$_{CT}$ | H5···O4 | 0.047 | +0.130 | 0.016 | +0.038 | 0.047 | +0.131 | 0.021 | +0.039 |
| | H6′′···O6 | 0.017 | +0.060 | 0.076 | +0.013 | 0.010 | +0.036 | 0.333 | +0.008 |
| | H3′′···O6c” | 0.026 | +0.093 | 0.040 | +0.022 | 0.029 | +0.104 | 0.041 | +0.025 |
| | H2′′···O4′′ | 0.017 | +0.057 | 0.088 | +0.013 | 0.022 | +0.075 | 0.058 | +0.017 |
| BCL*a1*$_{TT}$ | H5···O4 | 0.047 | +0.134 | 0.016 | +0.039 | 0.049 | +0.137 | 0.021 | +0.041 |
| | H6′′···O6 | 0.009 | +0.030 | 0.424 | +0.007 | – | – | – | – |
| | H6···O6c” | 0.009 | +0.033 | 0.152 | +0.007 | – | – | – | – |
| | H3′′···O6c” | 0.032 | +0.112 | 0.043 | +0.027 | 0.030 | +0.106 | 0.042 | +0.025 |
| | H4′′···O2′′ | 0.017 | +0.057 | 0.090 | +0.013 | 0.023 | +0.079 | 0.056 | +0.018 |
| | H6···O7 | – | – | – | – | 0.020 | +0.091 | 1.424 | +0.020 |
| BCL*a2*$_{TT}$ | H5···O4 | 0.047 | +0.134 | 0.016 | +0.039 | 0.049 | +0.137 | 0.021 | +0.041 |
| | H6′′···O6 | 0.010 | +0.034 | 0.376 | +0.008 | – | – | – | – |
| | H6···O6c” | 0.011 | +0.042 | 0.107 | +0.009 | – | – | – | – |
| | H3′′···O6c” | 0.032 | +0.113 | 0.044 | +0.028 | 0.030 | +0.105 | 0.042 | +0.025 |
| | H4′′···O2′′ | 0.017 | +0.057 | 0.090 | +0.013 | 0.023 | +0.078 | 0.056 | +0.018 |
| | H6···O7 | – | – | – | – | 0.020 | +0.091 | 1.494 | +0.020 |

[a] Atoms pair involved in the hydrogen bond interaction.

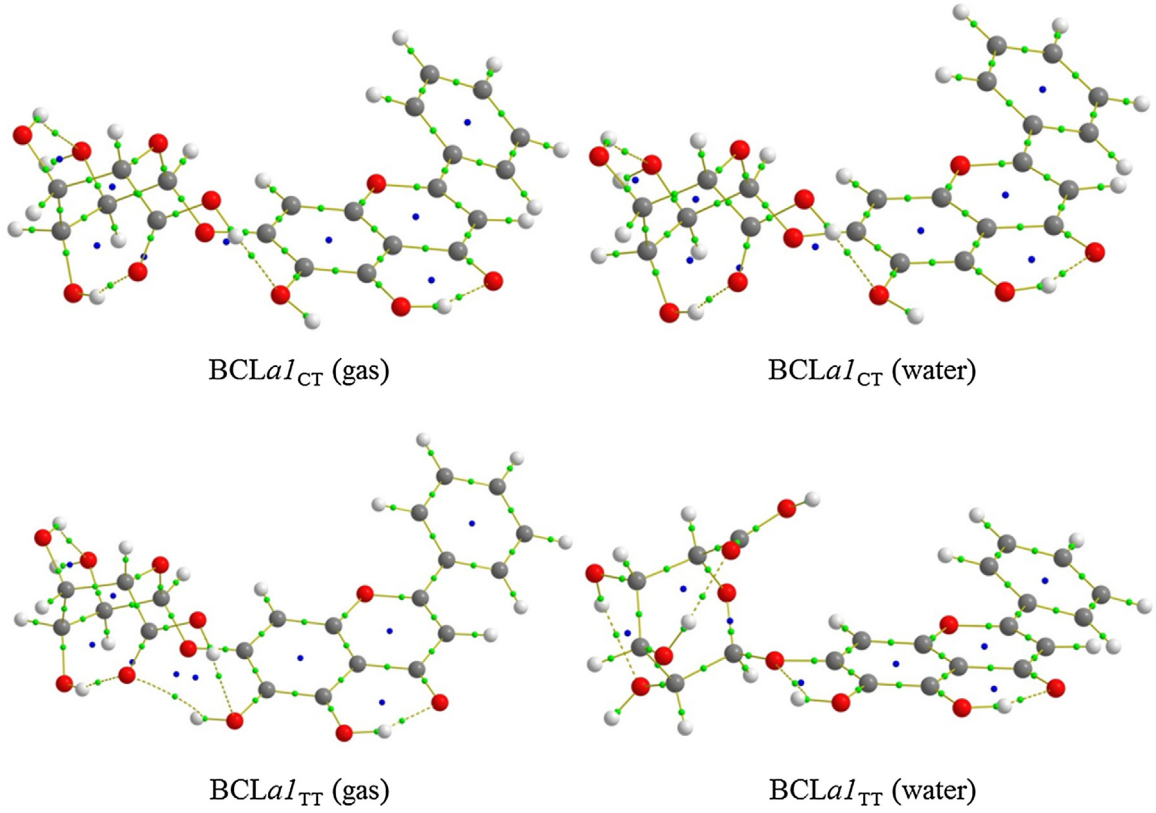


**Fig. 4.** AIM topology graphs of BCL*a1*$_{CT}$ and BCL*a1*$_{TT}$ conformers optimized in gas phase and in aqueous solution at B3LYP/6-311++G** theory level.

to the possible formation of IMHB interactions involving the OH groups of ring A (even C6—OH···O—C5). These IMHB interactions have been previously reported for baicalein [42]. Besides, Marković et al. [41] reported that there are three HBs present in the baicalein structure (even C6—OH···O—C5). Contrary to expectations, our data do not suggest the presence of an IMHB between the H6 and O5 atoms. Although the geometrical parameters (for example: the H6···O5 distance is 2.146 Å and the O6—H6···O5 angle is 113.5° in BCL*a1*$_{CT}$ in gas phase) are within the values accepted for HB, the topological analysis of BCL conformers with a cis configuration of the $\tau_5$ angle denotes the absence of BCP and bond path between the H6 and O5 atoms. Moreover, no RCP was found within the quasi-

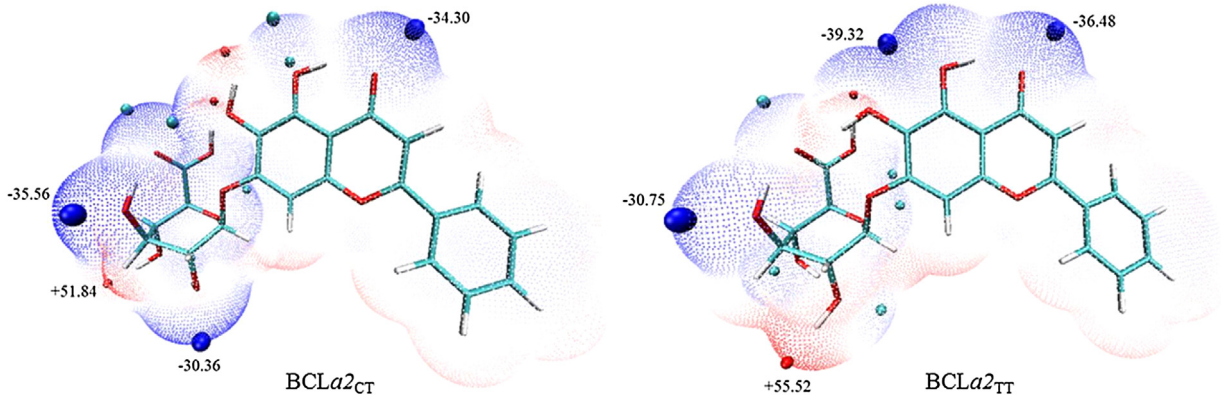


**Fig. 5.** Molecular electrostatic potentials mapped along the van der Waals surface of BCL$a2_{CT}$ and BCL$a2_{TT}$ conformers optimized in gas phase at B3LYP/6-311++G** theory level.

ring formed by the C6—OH···O—C5 bond. This fact may be explained considering the hybridization of the O5 atom. The strong HB formed between H5 and O4 atoms lead to the two lone pairs of O5 located in the $sp^3$ hybridized orbitals are above and below to the plane of the flavan nucleus. This fact is in concordance with the two minima observed above and below to the plane of the flavan nucleus in the MEP of BCL$a2_{CT}$ conformer (Fig. 5). The hypothesis of the absence of an IMHB between the H6 and O5 atoms is supported by the fact that the lone pairs of O5 atom and the H6 atom are not coplanar.

### 3.5. Molecular electrostatic potential analysis

Molecular electrostatic potential (MEP) closely correlates with electron density distribution and is a very useful descriptor for predicting favorable sites of electrophilic and nucleophilic reactions or revealing preferential sites of electrostatically dominated non-covalent interactions [46]. The MEP minima lower than −10 and maxima higher than +30 on the van der Waals (vdW) surface (in kcal $mol^{-1}$) of all BCL conformers calculated using the Multiwfn program are listed in Table S1. The MEPs mapped along the vdW surface of BCL$a2_{CT}$ and BCL$a2_{TT}$ conformers optimized in gas phase were selected for comparative purposes (Fig. 5). Their homologous structures with the phenyl in 20° show similar MEPs. The BCL$a2_{CT}$ and BCL$a2_{TT}$ conformers reoptimized in aqueous solution show similar MEPs. The blue color reveals very negative MEP region on the vdW surface, thus implying possible site for electrophilic attack. The red regions correspond to very positive MEP part of the vdW surface, thus expecting to be vulnerable sites for the nucleophilic attack. The color scale of the map ranges from −35.55 (blue) to +51.84 (red) in the BCL$a2_{CT}$ conformer in gas phase, but this range is particular for each conformer taking into account the MEP analysis results (Table S1). The local maxima higher than +40, minima lower than −30 and minima from −10 to −30 of MEP on the vdW surface are represented as red, blue and cyan spheres, respectively. The most relevant values of maxima (one) and minima (three) are labeled (Fig. 5).

In general trends, the MEP minima and maximum values on the vdW surface involves the substituents of the rings A and C and the glucuronide unit (not ring B). The relative position of the glucuronide unit and the ring B respect to the central rings doesn't affect the MEP, but the arrangement of the OH groups produces significant changes in the MEP. As expected, the MEP minima values on the vdW surface are located near the lone pair of the oxygen atoms and should be the most favorable site for interacting with positively charged species. On the contrary, the MEP maximum values on the vdW surface are found in front of the hydrogen atoms of the hydroxyl groups, thus indicating its strong capacity to attract negatively charged atoms electrostatically. In the present work, we focused on the characterization of the minima on the vdW surface (location and value) of BCL conformers because the antioxidant activity of baicalin in biological systems may be attributed to its chelating metal ion capacity. Despite the poor solubility of baicalin in water [7], this solvent was selected considering that it is the main component in biological fluids. After reoptimization in aqueous medium, the maximum values (positives) increased, whereas the minimum values (negatives) decreased. These findings suggest a higher reactivity of all BCL conformers in aqueous solution. For BCL$a2_{CT}$ the global surface minimum is located near the O3″ atom, whereas for BCL$a2_{TT}$ is located between the O5 and O6 atoms (of the hydroxyl substituents). In both cases, the second minimum is located near the oxygen of the carbonyl group of the flavan nucleus (O=C4) and may be attributed to the lone pair of O4 located in the $sp^2$ hybridized orbital not involved in the C5—OH···O=C4 bond. This fact explains the coplanarity of this minimum with the carbonyl group of the flavan nucleus. The results indicate that the arrangement trans of the OH 6 (ring A) generate a global surface minima in the BCL$a2_{TT}$ that is stronger than that in the BCL$a2_{CT}$ (Table S1). As spected, the aqueous solvent enhances the difference between the global minimum of BCL$a2_{TT}$ and BCL$a2_{CT}$. These findings, and the fact that the conformer BCL$a2_{TT}$ (or BCL$a1_{TT}$) is more stable and has more relative population than BCL$a2_{CT}$ (or BCL$a1_{CT}$), suggest that the conformers that show the arrangement trans of the OH 6 (ring A) are the most favorable conformers for interacting with positively charged species (such as metal ions) in aqueous solution (such as biological fluids).

### 3.6. Frontier molecular orbitals analysis

The highest occupied molecular orbital (HOMO) and the lowest unoccupied molecular orbital (LUMO) are useful descriptors in studying chemical stability of molecules. The energy of HOMO and LUMO characterize the ability of electron donating and accepting, respectively. The HOMO-LUMO gap helps to characterize the chemical reactivity and kinetic stability of the molecule [40,46]. The HOMO and LUMO energies and the corresponding HOMO-LUMO gap of all BCL conformers (optimized in gas phase and in aqueous solution) have been calculated at the B3LYP/6-311++G** level (Table 6). The HOMO-LUMO gap of BCL conformers is very similar to those of apigenin (4.09 eV) and luteolin (3.90 eV) flavonoids [39]. These low gap values reflect the chemical activity of BCL conformers. The most active conformers are BCL$a2_{TT}$ and BCL$a1_{TT}$ in gas phase and in aqueous solution. The intramolecular charge transfer interaction that takes place within the molecule is responsible for their activity [40]. The solvent effect slightly decreases the energy of

**Table 6**
HOMO and LUMO energies and HOMO-LUMO gap (ΔE) of the BCL conformers optimized in gas phase and in aqueous solution at B3LYP/6-311++G** theory level.

| Conformer | Gas phase | | | Aqueous solution | | | ΔE [c] |
|---|---|---|---|---|---|---|---|
| | HOMO | LUMO | ΔE [a] | HOMO | LUMO | ΔE [b] | |
| BCL$a2_{CT}$ | −6.378 | −2.481 | 3.897 | −6.312 | −2.420 | 3.892 | −0.005 |
| BCL$a1_{CT}$ | −6.406 | −2.510 | 3.896 | −6.321 | −2.417 | 3.904 | 0.008 |
| BCL$a1_{TT}$ | −6.184 | −2.382 | 3.802 | −6.225 | −2.383 | 3.842 | 0.040 |
| BCL$a2_{TT}$ | −6.203 | −2.407 | 3.796 | −6.225 | −2.384 | 3.841 | 0.045 |
| BCL$b1_{CC}$ | −6.543 | −2.605 | 3.938 | −6.422 | −2.477 | 3.945 | 0.007 |
| BCL$b2_{CC}$ | −6.656 | −2.700 | 3.956 | −6.470 | −2.505 | 3.965 | 0.009 |
| BCL$c1_{CC}$ | −6.546 | −2.612 | 3.934 | −6.383 | −2.469 | 3.914 | −0.020 |
| BCL$c1_{CT}$ | −6.414 | −2.550 | 3.864 | −6.347 | −2.455 | 3.892 | 0.028 |

[a] HOMO–LUMO gap in gas phase, expressed in electron-volts (eV).
[b] HOMO–LUMO gap in aqueous solution, expressed in electron-volts (eV).
[c] Solution-vacuum gap energy difference, expressed in electron-volts (eV).

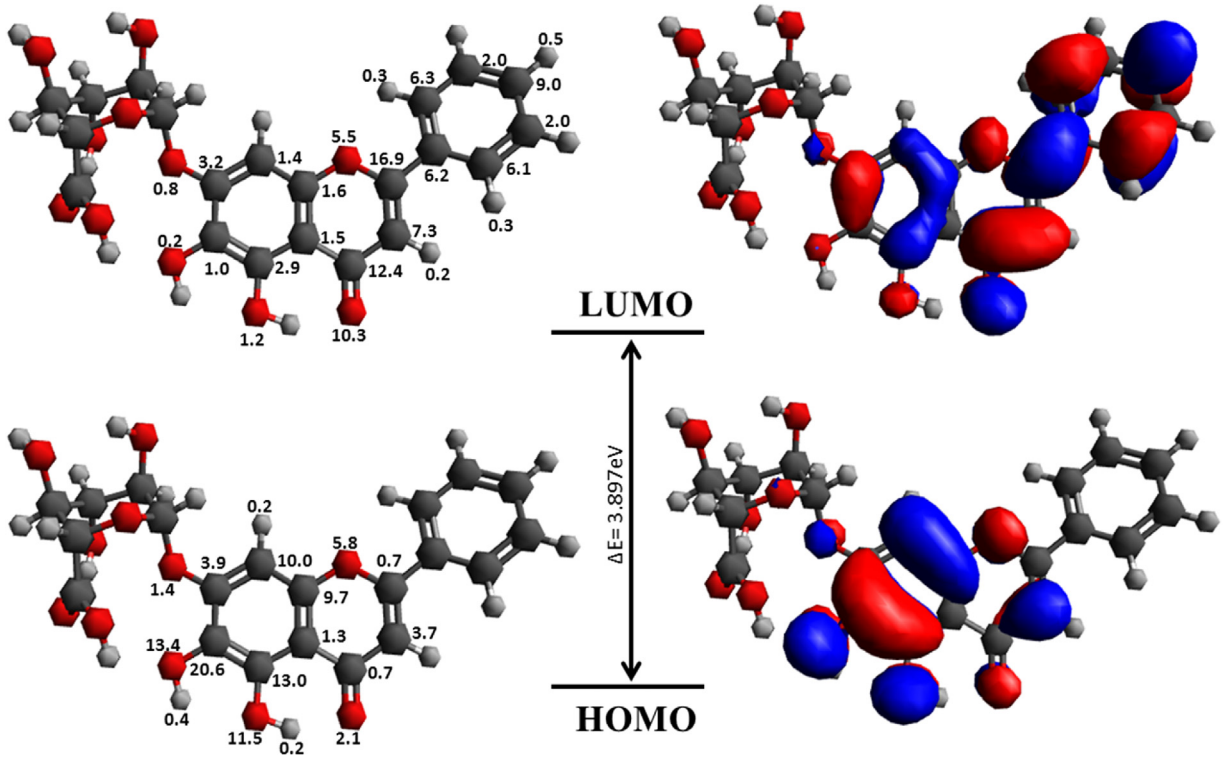


**Fig. 6.** Contour plots and mayor atom contributions (expressed in percentage) of HOMO an LUMO of the most stable conformer optimized in gas phase at B3LYP/6-311++G** theory level (BCL$a2_{CT}$).

the frontier molecular orbitals. Nevertheless, the gap values show no modifications and the solution-vacuum gap energy difference is negligible in most cases (except in BCL$a2_{TT}$ and BCL$a1_{TT}$ conformers). In general trends, the aqueous solvent does not affect the stability and reactivity of the BCL conformers, but in BCL conformers with a trans configuration of the $\tau_5$ angle (BCL$a2_{TT}$ and BCL$a1_{TT}$) the solution-vacuum gap energy difference suggest an enhanced stability of these conformers in aqueous solution. These findings are in agreement with the energetic order and relative population (Table 3) and with the AIM analysis results.

The frontier molecular orbitals (HOMO or LUMO) of all BCL conformers (optimized in gas phase and in aqueous solution) were visualized with Avogadro for comparative purposes and we found that they show no significant differences. HOMO (or LUMO) orbital has the same spatial arrangements in all BCL conformers, being almost identical. This fact led us to select the BCL$a2_{CT}$ conformer (the most stable conformer in gas phase) to study the composition of HOMO and LUMO employing the Multiwfn program (by the Becke method). Fig. 6 shows orbital isosurfaces and mayor atom contributions in BCL$a2_{CT}$. The frontier molecular orbitals of BCL$a2_{CT}$ principally come from to the flavan nucleus (not from the glucuronide unit). The HOMO is distributed over the rings A and C (no ring B), but mainly localized on the C5—C6 and C8—C9 bonds. The O6, O5 and O1 atoms have contributions of 13.4%, 11.5% and 5.8% to HOMO. The LUMO is distributed along the flavan nucleus (including ring B), but mainly localized on the C3—C4 and C2—C1′ bonds. The C4′, C2′, C6′, O4 and O1 atoms have contributions of 9%, 6.3%, 6.1%, 10.3% and 5.5% to LUMO. The contributions mentioned previously are the main contributions (>5%), but other contributions (>0.1%) slightly delocalized to the rest of the molecule are marked in Fig. 6. The HOMO of baicalin molecule is π-orbital, whereas the LUMO is π*-orbital. The spatial arrangement of the FMOs of baicalin is very similar to those of baicalein [41] and slightly different from those of apigenin and luteolin flavonoids [39,40].

## 4. Conclusions

The study of the conformational space of baicalin allowed us to determine the coexistence of eight BCL conformers in gas phase and five BCL conformers in aqueous solution. These conformers were optimized at B3LYP/6-311++G** theory level. The most stable BCL conformers involved the *a* ($\tau_1 = -35.31^\circ$ in gas phase and $15.48^\circ$ in aqueous solution) and *b* ($\tau_1 = -122.07^\circ$ in gas phase and $-108.35^\circ$ in aqueous solution) groups. The effect of aqueous solvent reduced the conformational space of baicalin and modified the stability order of BCL conformers. No significant changes were observed in the geometry of the conformers after reoptimization in aqueous medium (except for BCL$a2_{TT}$ and BCL$a1_{TT}$). Surprisingly, BCL$a2_{TT}$ and BCL$a1_{TT}$ conformers have low stability in gas phase and very high stability in aqueous solution, due to a modification in the $\tau_1$ angle. This modification was successfully explained attending the changes in the HB interactions that occur in the region around the OH located in position 6 of ring A. The MEP analysis results indicate that the arrangement trans of the OH 6 generate a global surface minima located between the oxygen atoms O5 and O6 of the hydroxyl substituents and that the aqueous solvent enhances the reactivity of BCL conformers. The FMO analysis results indicate that BCL conformers are reactive species capable to interact with other molecules. The BCL$a2_{TT}$ and BCL$a1_{TT}$ conformers that show the arrangement trans of the OH 6 (ring A) are the most favorable conformers for interacting with positively charged species (such as metal ions) in aqueous media (such as biological fluids).

## Acknowledgements

This work was supported by UNCAus, UNLP, CONICET, CICPBA, PIP (0611) and ANPCyT (PICT 2013-0569), Argentina. NBO and EGF are research fellows of CONICET. PAMW is a research fellow of CICPBA, Argentina. JJMM is fellowship holder from CONICET.

## Appendix A. Supplementary data

Supplementary data associated with this article can be found, in the online version, at http://dx.doi.org/10.1016/j.jmgm.2017.07.007.

## References

[1] S. Kumar, A.K. Pandey, Chemistry and biological activities of flavonoids: an overview, ScientificWorld J. 2013 (2013) 1–16.
[2] D. Sanna, V. Ugone, G. Lubinu, G. Micera, E. Garribba, Behavior of the potential antitumor $V^{IV}O$ complexes formed by flavonoid ligands. 1. Coordination modes and geometry in solution and at the physiological pH, J. Inorg. Biochem. 140 (2014) 173–184.
[3] D. Amić, B. Lučić, Reliability of bond dissociation enthalpy calculated by the PM6 method and experimental TEAC values in antiradical QSAR of flavonoids, Bioorg. Med. Chem. 18 (2010) 28–35.
[4] M.M. Kasprzak, A. Erxleben, J. Ochocki, Properties and applications of flavonoid metal complexes, RSC Adv. 5 (2015) 45853–45877.
[5] C.A. Perez, Y. Wei, M. Guo, Iron-binding and anti-Fenton properties of baicalein and baicalin, J. Inorg. Biochem. 103 (2009) 326–332.
[6] M. Wolniak, J. Oszmiański, I. Wawer, Solid-state NMR studies and DFT calculations of flavonoids: baicalein: baicalin and wogonoside, Magn. Reson. Chem. 46 (2008) 215–225.
[7] L. Zhao, Y. Wei, Y. Huang, B. He, Y. Zhou, J. Fu, Nanoemulsion improves the oral bioavailability of baicalin in rats: in vitro and in vivo evaluation, Int. J. Nanomed. 8 (2013) 3769–3779.
[8] Z.Y. Cheng, X. Tian, J. Gao, H.M. Li, L.J. Jia, H.L. Qiao, Contribution of baicalin on the plasma protein binding displacement and CYP3A activity inhibition to the pharmacokinetic changes of nifedipine in rats *In vivo* and *In vitro*, PLoS One 9 (2014) 1–8.
[9] N.R. Srinivas, Baicalin, an emerging multi-therapeutic agent: pharmacodynamics, pharmacokinetics, and considerations from drug development perspectives, Xenobiotica 40 (2010) 357–367.
[10] S. Yang, Y. Fu, X. Wu, Z. Zhou, J. Xu, X. Zeng, N. Kuang, Y. Zeng, Baicalin prevents Candida albicans infections via increasing its apoptosis rate, Biochem. Biophys. Res. Commun. 451 (2014) 36–41.
[11] Y. Huang, S.Y. Tsang, X. Yao, Z.Y. Chen, Biological properties of baicalein in cardiovascular system, Curr. Drug Targets Cardiovasc. Haematol. Disord. 5 (2005) 177–184.
[12] J.a. Zhang, Z. Yin, L.w. Ma, Z.q. Yin, Y.y. Hu, Y. Xu, D. Wu, F. Permatasari, D. Luo, B.r. Zhou, The protective effect of baicalin against UVB irradiation induced photoaging: an in vitro and In vivo study, PLoS One 9 (2014) 1–13.
[13] X. Wang, Y. Zhao, X. Zhong, Protective effects of baicalin on decidua cells of LPS-induced mice abortion, J. Immunol. Res. 2014 (2014) 1–6.
[14] X. Wei, J. Yang, C. Wu, Anxiolytic effect of baicalin in mice, Asian J. Tradit. Med. 1 (2006) 3–4.
[15] J. Yang, X. Yang, M. Li, Baicalin, a natural compound, promotes regulatory T cell differentiation. BMC Complement, Altern. Med. 12 (2012) 1–7.
[16] X. Yang, J. Yang, H. Zou, Baicalin inhibits IL-17-mediated joint inflammation in murine adjuvant-induced arthritis, Clin. Dev. Immunol. 2013 (2013) 1–8.
[17] S.M. Wu, H.Y. Wu, Y.J. Wu, L. Liu, R.P. Cai, Y.J. Xu, Effects of Baicalin and Ligustrazine on airway inflammation and remodeling and underlying mechanism in asthmatic rats, Adv. Biosci. Biotechnol. 3 (2012) 585–591.
[18] A.R. Kim, S.N. Kim, I.K. Jung, H.H. Kim, Y.H. Park, W.S. Park, The inhibitory effect of scutellaria baicalensis extract and its active compound baicalin, on the translocation of the androgen receptor with implications for preventing androgenetic alopecia, Planta Med. 80 (2014) 153–158.
[19] C. Guo, X. Chen, P. Xiong, Baicalin suppresses iron accumulation after substantia nigra injury: relationship between iron concentration and transferrin expression, Neural Regen. Res. 9 (2014) 630–636.
[20] T. Tarragó, N. Kichik, B. Claasen, R. Prades, M. Teixidó, E. Giralt, Baicalin, a prodrug able to reach the CNS, is a prolyl oligopeptidase inhibitor, Bioorg. Med. Chem. 16 (2008) 7516–7524.
[21] J. Dou, L. Chen, G. Xu, L. Zhang, H. Zhou, H. Wang, Z. Su, M. Ke, Q. Guo, C. Zhou, Effects of baicalein on Sendai virus in vivo are linked to serum baicalin and its inhibition of hemagglutinin-neuraminidase, Arch. Virol. 156 (2011) 793–801.
[22] Q. Liu, L. Qiu, Y. Wang, G. Lv, G. Liu, S. Wang, J. Lin, Solvent effect on molecular structure IR spectra, thermodynamic properties and chemical stability of zoledronic acid: DFT study, J. Mol. Mod. 22 (2016) 1–11.
[23] Q. Dai, X. Lei, J. Yang, Q. Cheng, C. Gao, H. Li, Crystal structure of baicalin, Acta Chim. Sinica 67 (2009) 2363–2367.
[24] J.J.P. Stewart, Optimization of parameters for semiempirical methods. I. Method, J. Comput. Chem. 10 (1989) 209–220.
[25] J.J.P. Stewart, Optimization of parameters for semiempirical methods. II. Applications, J. Comput. Chem. 10 (1989) 221–264.
[26] P. Hohenberg, W. Kohn, Inhomogeneous electron gas, Phys. Rev. 136 (1964) B864–B871.
[27] W. Kohn, L.J. Sham, Self-Consistent equations including exchange and correlation effects, Phys. Rev. 140 (1965) A1133–A1138.
[28] R.G. Parr, W. Yang, Density Functional Theory of Atoms and Molecules, Oxford University Press Clarendon Press, Oxford; New York, 1989.
[29] M.J. Frisch, et al., Gaussian 09, Revision B.01, Gaussian, Inc, Wallingford CT, 2009.
[30] A.D. Becke, Density-functional thermochemistry. III. The role of exact exchange, J. Chem. Phys. 98 (1993) 5648–5652.
[31] R.M. Lobayan, E.N. Bentz, A.H. Jubert, A.B. Pomilio, Structural and electronic properties of Z isomers of ($4\alpha \rightarrow 6''$, $2\alpha \rightarrow O \rightarrow 1''$)-phenylflavans substituted with R = H, OH and OCH calculated in aqueous solution with PCM solvation model, J. Mol. Mod. 18 (2012) 1667–1676.
[32] E.N. Bentz, A.B. Pomilio, R.M. Lobayan, Structure and electronic properties of (+)-catechin: aqueous solvent effects, J. Mol. Mod. 20 (2014) 1–13.
[33] G. Scalmani, M.J. Frisch, Continuous surface charge polarizable continuum models of solvation. I. General formalism, J. Chem. Phys. 132 (2010) 1–15.
[34] T. Lu, F. Chen, Multiwfn: a multifunctional wavefunction analyzer, J. Comput. Chem. 33 (2012) 580–592.
[35] W. Humphrey, A. Dalke, K. Schulten, VMD: visual molecular dynamics, J. Mol. Graph. 14 (1996) 33–38.
[36] M.D. Hanwell, D.E. Curtis, D.C. Lonie, T. Vandermeersch, E. Zurek, G.R. Hutchison, Avogadro: an advanced semantic chemical editor visualization, and analysis platform, J. Cheminform. 4 (2012) 1–17.
[37] R.F.W. Bader, Atoms in Molecules: a Quantum Theory, Oxford University Press, Oxford, 1995.
[38] T.A. Keith, AIMAll (Version 17.01.25), TK Gristmill Software, Overland Park KS, USA, 2017.
[39] A. Amat, F. De Angelis, A. Sgamellotti, S. Fantacci, Theoretical investigation of the structural and electronic properties of luteolin: apigenin and their deprotonated species, J. Mol. Struct. THEOCHEM 868 (2008) 12–21.
[40] G. Mariappan, N. Sundaraganesan, S. Manoharan, The spectroscopic properties of anticancer drug Apigenin investigated by using DFT calculations, FT-IR: FT-Raman and NMR analysis, Spectrochim. Acta A Mol. Biomol. Spectrosc. 95 (2012) 86–99.
[41] Z.S. Marković, J.M. Dimitrić-Marković, D. Milenković, N. Filipović, Structural and electronic features of baicalein and its radicals, Monatsh. Chem. 142 (2011) 145–152.
[42] M. Rossi, R. Meyer, P. Constantinou, F. Caruso, D. Castelbuono, M. O'Brien, V. Narasimhan, Molecular structure and activity toward DNA of baicalein, a flavone constituent of the asian herbal medicine Sho-saiko-to, J. Nat. Prod. 64 (2001) 26–31.
[43] Y.Z. Zheng, Y. Zhou, Q. Liang, D.F. Chen, R. Guo, C.L. Xiong, X.J. Xu, Z.N. Zhang, Z.J. Huang, Solvent effects on the intramolecular hydrogen-bond and anti-oxidative properties of apigenin: a DFT approach, Dyes Pigm. 141 (2017) 179–187.

[44] B.K. Paul, N. Guchhait, Geometrical criteria versus quantum chemical criteria for assessment of intramolecular hydrogen bond (IMHB) interaction: a computational comparison into the effect of chlorine substitution on IMHB of salicylic acid in its lowest energy ground state conformer, Chem. Phys. 412 (2013) 58–67.
[45] A. Ganguly, B.K. Paul, S. Ghosh, N. Guchhait, A computational acumen into the relative applicability of geometrical and quantum chemical criteria in assessing intramolecular hydrogen bonding (IMHB) interaction: 5-Halosalicylic acids as representative examples, Comp. Theor. Chem. 1018 (2013) 102–114.
[46] Y. Tao, X. Li, L. Han, W. Zhang, Z. Liu, Spectroscopy (FT-IR, FT-Raman), hydrogen bonding, electrostatic potential and HOMO-LUMO analysis of tioxolone based on DFT calculations, J. Mol. Struct. 1121 (2016) 188–195.